Current Source LCC Resonant Converter for an EDM Power Supply

Rosario Casanueva, Luis A. Chiquito, Francisco J. Azcondo, Salvador Bracho
University of Cantabria
Dept. of Electronics Technology, Systems and Automation Engineering
Av. de los Castros, s/n.
39005 Santander, SPAIN
{charo, lacd, azcondo, bracho}@teisa.unican.es

Abstract – **In this paper, the design of a low size power supply prototype for Electrical Discharge Machining is presented. The system is a dc to dc LCC resonant converter whose switching frequency is tuned at the natural resonant frequency where the converter tends to act as a current source. In this way, two effects are achieved: 1) the necessary over-voltage, first to ionize the dielectric and then to establish the electric arc is generated and 2) a constant current is supplied during the erosion of the workpiece, providing the circuit with inherent protection under short circuit conditions. The output voltage is intended to be adjusted by an external system that controls the arc distance.**

I. INTRODUCTION

Electrical Discharge Machining (EDM) is an electrothermal process. EDM uses an electrode positioned at a fixed small distance (spark gap) above the workpiece, both submerged in a dielectric fluid. A pulsating dc power supply or EDM generator applies voltage pulses between the electrode and workpiece, generating sparks or current conduction through the gap. Each spark results in localized heating that melts a small area of the workpiece surface. (Fig. 1).

Basically, an EDM system consists of the following main components [1],[2]:

- Workpiece and electrode.
- Dielectric fluid.
- DC power supply.
- Servomechanism, to maintain a constant gap.

Traditional EDM power supplies convert the energy at low frequency, directly from the utility line and they are able to deal with a wide spectrum of output power. The EDM power supply must achieve high voltage to generate the spark and large current to maintain the ion column. To achieve this, large and heavy transformers and inductances are required.

Our proposal uses the characteristics of power mosfet devices and resonant converters to achieve a compact solution to be applied in field machining to provide maintenance and repair services to nuclear or traditional power plants or any industrial plant. EDM is an adequate technique to perform machining tasks in nuclear plants because it does not produce chips that could cause damage to reactor components. In EDM, micron size particles are immediately flushed away with the dielectric fluid. In addition, it is ideally suited for underwater applications.

Since power mosfets accept large repetitive peak current because of the positive temperature coefficient of their on-state resistance, they are suitable to be used under overload conditions during the dielectric breakdown transition. In addition, their high switching frequency allows the reduction of the inductance and transformer size.

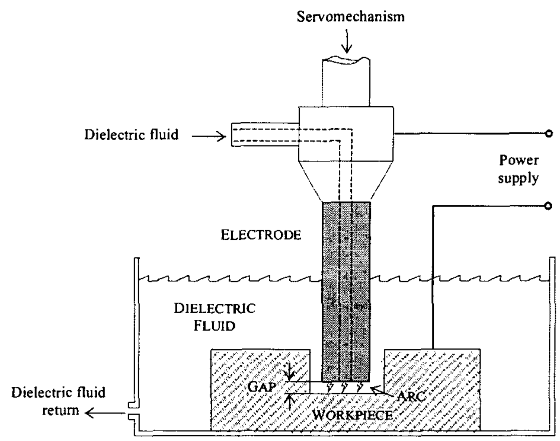

Fig. 1. Basic EDM process.

II. PROPOSED EDM SUPPLY

The EDM generator must provide the voltage and current waveforms [3] as depicted in Fig. 2.

The machining frequency is specified to be up to 10 kHz. During the on-time the generator applies the potential difference between the electrode and workpiece to generate and sustain the current through the arc, and during the off-time the output power is interrupted, causing the arc current to drop down to zero. The generator must increase the voltage between the electrode and the workpiece, typically up to 200 V, to ionize the dielectric.

Based on experimental measurements, during the on-time, after the dielectric breakdown has occurred, the converter load, that is, the ion column, is modeled as a resistance.

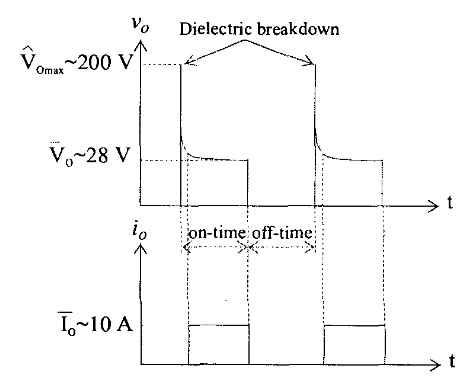

Fig. 2. Specified EDM waveforms.

Once the dielectric resistance is overcome, the generator must sustain an operating point where the arc voltage is around 28 V and the current is kept around 10 A until the end of the on-time.

The proposed solution for the EDM requirements is a full-bridge LCC resonant converter operating at a switching frequency of 200 kHz, used as a current source and it is shown in Fig. 3.

Resonant converters have well-known advantages for high frequency dc to dc power supplies because they result in small size, light weight and highly efficient systems since high frequency operation minimizes the size of the magnetic components.

LCC resonant converters are able to achieve the required voltage for the dielectric breakdown, and working above the resonant frequency, current lags voltage so this topology achieves zero voltage switching, that is, transistors turn on at zero voltage, resulting in minimum switching losses.

The full bridge configuration has been chosen because of its capability of converting high power.

As the continuous change in the gap distance may lead to load changes from open to short circuit conditions, the resonant inverter is designed as a current source to provide the system with inherent protection under short circuit conditions. The open circuit fault must be limited by an over-voltage protection.

The design sequence of the LCC resonant inverter is oriented to achieve the dielectric breakdown and current stabilization while limiting maximum stress on the components by design.

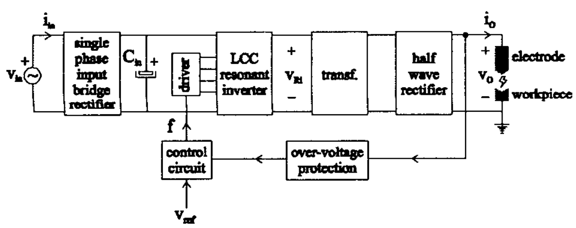

Fig. 3. Basic block diagram of the EDM power supply using a LCC resonant converter.

III. CURRENT SOURCE, LCC RESONANT INVERTER DESIGN

Fig. 4 (a) shows the full-bridge resonant inverter. The circuit input is the rectified utility line voltage, the full bridge topology applies a square wave voltage, v_{AB}, to the resonant network.

The waveforms in the resonant circuit are nearly sine waves, so essentially a sine wave appears at v_{AB}. This analysis method is called the fundamental approximation [4], the first harmonic of v_{AB} is applied to the resonant circuit as shown in Fig. 4 (b).

The analysis of this circuit is based on the following parameters:

- The equivalent resistance, R_i, that models the transformer, the half-wave rectifier and the gap resistance.

- The ratio of the capacitances,

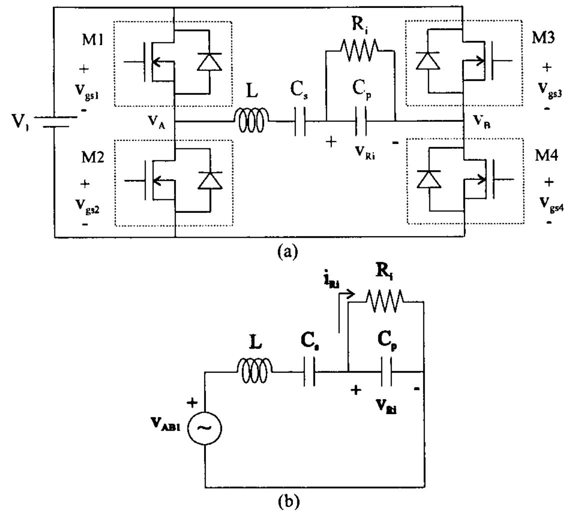

Fig. 4. (a) Full bridge LCC resonant inverter. (b) Simplified circuit.

$$A = \frac{C_p}{C_s} \tag{1}$$

- The parallel resonant frequency,

$$\omega_p = \frac{1}{\sqrt{LC_p}} \tag{2}$$

- The characteristic impedance at ω_p,

$$Z_p = \omega_p L = \frac{1}{\omega_p C_p} \tag{3}$$

- The parallel quality factor,

$$Q_p = \frac{R_i}{Z_p} \tag{4}$$

To design the LCC resonant inverter as a current source, the expression of the current amplitude through the equivalent resistance [5] is analyzed,

$$\hat{I}_{Ri} = \frac{4V_I}{\pi Z_p Q_p}\sqrt{\frac{1+Q_p^2\left(\frac{\omega}{\omega_p}\right)^2}{1+\left[\frac{1}{Q_p}\left(\frac{\omega}{\omega_p}-\frac{\omega_p}{\omega}A\right)\left(1+Q_p^2\left(\frac{\omega}{\omega_p}\right)^2\right)-Q_p\frac{\omega}{\omega_p}\right]^2}} \tag{5}$$

Fig. 5 shows this current as a function of the frequency for different parallel quality factors, that is, for different loads, from short circuit to open circuit. Expression (5) has no dependence on the load at the frequency,

$$\omega = \omega_p\sqrt{A+1} = \omega_0 \tag{6}$$

where ω_0 is the unloaded natural resonant frequency of the LCC circuit.

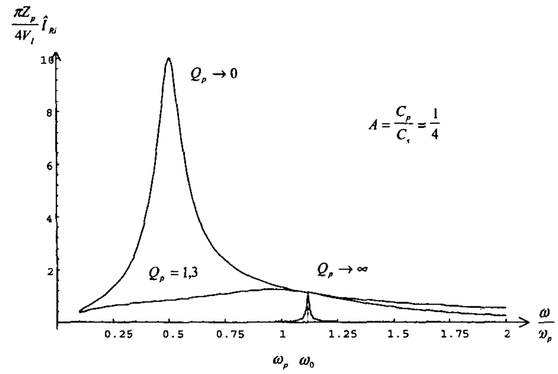

Fig. 5. Normalized current through R_i as a function of the switching frequency for different parallel quality factors.

Thus, at this frequency, the current amplitude through the equivalent resistance becomes,

$$\hat{I}_{Ri}\Big|_{\omega=\omega_0} = \frac{4V_I}{\pi Z_p}\sqrt{A+1} \tag{7}$$

for any value of R_i.

From (3), (6) and (7) the parallel capacitance is obtained for a given $\hat{I}_{Ri}$.

$$C_p = \frac{\hat{I}_{Ri}\big|_{\omega=\omega_0}}{8V_I f_0} \tag{8}$$

Taking into account the inverter parameters (1) and (3), the expressions of the series capacitance and the inductor are given by,

$$C_s = \frac{C_p}{A} = \frac{\hat{I}_{Ri}\big|_{\omega=\omega_0}}{8AV_I f_0} \tag{9}$$

$$L = \frac{2(A+1)V_I}{\pi^2 f_0 \hat{I}_{Ri}\big|_{\omega=\omega_0}} \tag{10}$$

These expressions depend on the input voltage, V_I, the resonant frequency, f_0, and the required equivalent resistance current amplitude, $\hat{I}_{Ri}$.

The transformer turns ratio, n, is calculated to meet the breakdown transition requirements by

$$n = \frac{\hat{V}_{Ri,\max}}{\hat{V}_{O,\max}} \tag{11}$$

where $\hat{V}_{O,max}$ is the specified peak output voltage, that is the breakdown voltage, and $\hat{V}_{Ri,max}$ is the maximum value of the peak voltage across R_i.

Thus, the equivalent resistance voltage amplitude is obtained by,

$$\hat{V}_{Ri} = n\sqrt{2}V_{Orms} \tag{12}$$

where V_{Orms} is the rms value of the on-state output voltage.

As a first approach the half-wave rectifier is considered with no conduction losses and no output filter is used. In this way, the equivalent resistance, which models the rectifier and the load, the current through it and the output resistance are finally obtained by,

$$R_i = \frac{\hat{V}_{Ri}^2}{2P_O} \tag{13}$$

$$\hat{I}_{Ri} = \frac{\hat{V}_{Ri}}{R_i} \tag{14}$$

$$R_O = \frac{R_i}{n^2} \tag{15}$$

The following steps summarize the design sequence:
- The input data: V_I, $\hat{V}_{Ri,max}$, V_{Orms}, $\hat{V}_{O,max}$, P_O, f, are collected.
- Using (11), the transformer turns ratio, n, is obtained.
- From (12) and (13) the peak equivalent resistance voltage and R_i, are calculated.
- Substitution of the resulting values of $\hat{V}_{Ri}$ and R_i into (14) yields the equivalent resistance current, $\hat{I}_{Ri}$.
- From (8), C_p is obtained, the closest standard value is chosen and the frequency, f, is re-calculated.
- A value of A is selected and using (9) and (10) the values of C_s and L are obtained.
- Finally, from (15) the value of the output resistance, R_O, which models the gap distance between the electrode and the workpiece is obtained.

IV. CONTROL DESIGN

A control circuit has been developed to establish the switching frequency of the resonant inverter slightly above ω_0 to fix the desired output current during the on-time. During the off-time, two solutions have been verified: 1) to fix the switching frequency well above ω_0, where the current through the load is as low as possible while transistors keep switching, so at the next machining pulse the dielectric breakdown is achieved minimizing the maximum stress on the components; 2) to turn off the power switches. The second solution has finally been adopted because it does not mean high stress on the components at the dielectric breakdown and it achieves lower overall losses than the first solution. It should be noted that the behavior of the LCC inverter is highly dependent on the load except if, for current source operation, the switching frequency is ω_0 and, at this frequency, the inverter is designed to supply the nominal output current.

The logic of the control circuit is implemented by means of a CPLD, which allows easy modification of the design, clocked by a 20 MHz crystal oscillator. This control circuit provides the driving signals to the power mosfets at the desired frequency. This frequency depends on the reference voltage, which is a square signal with controlled pulse width to adjust the output power at 10 kHz, the specified machining frequency. If the over-voltage protection is activated during the on-time, the power mosfets are turned off until the next machining pulse.

The control circuit operates in open loop because the practical tuning of ω is good enough, the control circuit is greatly simplified and the control signals are not perturbed by the power section.

V. EXPERIMENTAL RESULTS

Some prototypes have been designed based on the techniques presented in this paper. First, the performance of the inverter was verified [6], the results confirm stable behavior under the control criteria of the inverter working at high frequency at the constant current operating point. The lastest prototypes include the transformer and the output rectifier. At present, preliminary results on the EDM system have been obtained. In this section the results of the dc-dc converter and the results of the EDM system are presented.

The resonant converter is designed with the sequence proposed in Section III and the following specifications:

main input supply voltage	$V_I = 280$ V,
maximum peak voltage across R_i	$\hat{V}_{Ri,max} = 1500$ V,
rms on-time output voltage	$V_{Orms} = 30$ V,
peak output voltage	$\hat{V}_{O,max} = 200$ V,
on-time output power	$P_O = 300$ W,
switching frequency	$f = 200$ kHz.

The resulting practical implementation circuit parameters are summarized below:

transformer turn ratio	$n = 7$,
voltage amplitude across R_i	$\hat{V}_{Ri} = 300$ V,
equivalent resistance	$R_i = 150\ \Omega$,
current amplitude through R_i	$\hat{I}_{Ri} = 2$ A,
parallel capacitance	$C_p = 4.7$ nF,
switching frequency	$f = 205$ kHz,
ratio of the capacitances	$A = 0.25$,
series capacitance	$C_s = 20$ nF,
resonant inductor	$L = 157\ \mu$H,
ouput resistance	$R_O = 3.3\ \Omega$.

The resonant inductor was wound on a Siemens ETD 59 core of N87 material with 20 turns with an air gap of 1.4 mm. The switching frequency was chosen to be 208 kHz, just above the resonant frequency, f_0. The transformer was wound on a Siemens ETD 59 core of N87 material with 21 turns on the primary and 3 turns on each secondary with an air gap of 0.04 mm. The output rectifier diodes were RHRP3060, 30 A hyperfast diodes with soft recovery characteristics. The high-frequency full-bridge MOSFET transistors selected were IRFP350 (400 V, 16 A, 0.3 Ω) and IR2111 circuits as drivers.

The circuit has been verified by emulating the gap resistance by means of an output resistor, R_O.

Fig. 6 shows the transistor's switching current and voltage at turn on transition, the reference voltage, v_{ref}, changes from 0 V to 4 V at 10 kHz. During the on-time the switching frequency is 208 kHz. As seen, transistors turn on at zero voltage, resulting in minimum switching losses.

Fig. 7 shows the experimental waveforms of the output current and voltage of the converter at full load, $R_O = 3.3$ Ω. The reference voltage changes from nominal operation to arc extinction and vice versa at 10 kHz. During the on-time the system provides an rms output current equal to 11.4 A and the rms output voltage is 37.3 V.

Even when the gap is greater than the desired gap distance, which may produce a load deviation from the nominal value, the power supply provides the specified current as shown in Fig. 8, where a load change has been emulated using an output resistor of 10 Ω (166% of full load). During the on-time, the rms output current is around 10.2 A and the rms output voltage is 93.2 V.

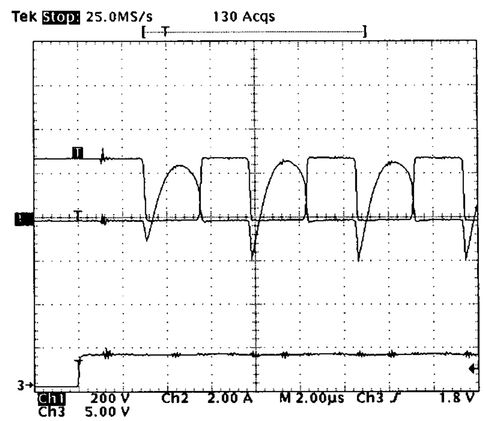

Fig. 6. Switching current and voltage at turn on transition.

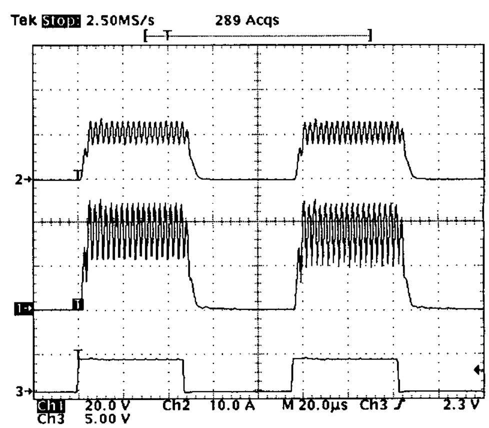

Fig. 7. Output current and voltage. Full load.

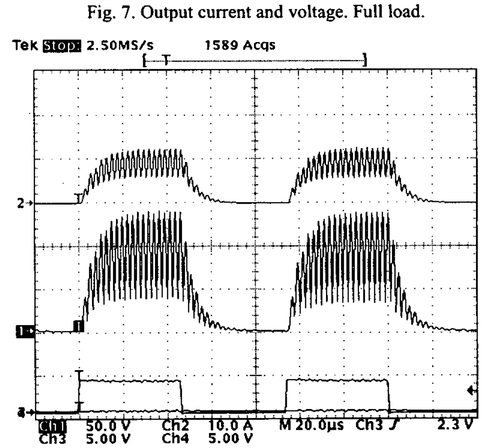

Fig. 8. Output current waveform. 166% of full load.

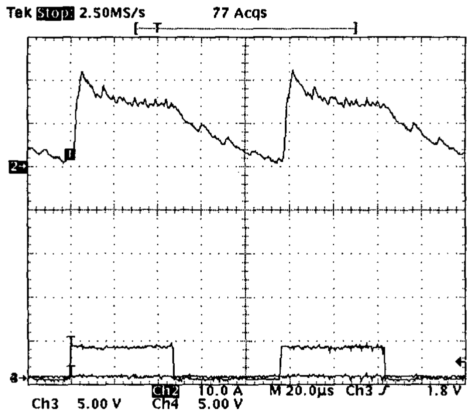

Fig. 9. Output current under short circuit conditions.

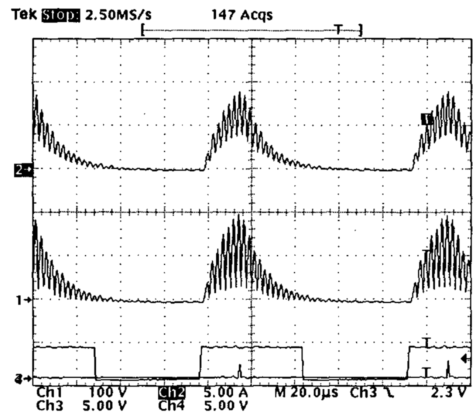

Fig. 10. Over-voltage condition.

Fig. 9 shows the output current under short circuit conditions. The output current is within the operation range even if the electrode and the workpiece were to contact somehow.

To verify the over-voltage protection circuit, an over-voltage condition was emulated by means of an output resistance of 20 Ω connected to the dc-dc converter. Fig. 10 shows the voltage on the primary side of the transformer, the output voltage, the reference voltage and the over-voltage signal. Once the over-voltage condition is detected the voltage drops until the next machining pulse.

The converter performance has been verified on an EDM operation. Table I shows the machining conditions and the generator setup for this experiment. A stainless steel plate is used as a workpiece. The graphite electrode is round and its size is 8 mm ∅ and 9 cm long with a flush hole of 3 mm ∅. The power supply used in the experiment is the actual prototype. Voltage pulses are applied between the electrode and the workpiece at 10 kHz and the pulse width of the discharge is 50 µs. The dielectric fluid is water flushed by using a jet directed against the arc gap. The gap size is 0.05 mm and, in this experiment, it was maintained constant manually. In the future, a servomechanism will control the gap distance. Electrode polarity has been chosen negative because it is used to machine holes, electrode wear is not a consideration and it achieves a higher metal removal rate. Positive polarity protects graphite electrodes from excessive wear but it would machine more slowly, a typical application is moldmaking.

TABLE I
EDM CONDITIONS

Machining Conditions	
Electrode	0.8 mm ∅ Graphite
Workpiece	INOX 316
Gap size	0.05 mm
Dielectric fluid	Water
Type of flushing	External
Generator Conditions	
Electrode polarity	Negative
Pulse width	50 µs
Duty cycle	50%

Fig. 11 shows the voltage and current waveforms provided by the circuit used as an EDM power supply. During the on-time the rms output current is around 12.6 A and the rms output voltage is ~19 V.

Fig. 12 and Fig. 13 show sparks in the machining process and the resulting cuts in the workpiece.

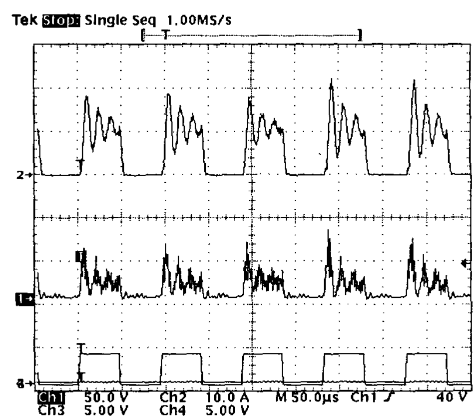

Fig. 11. Current and voltage between the electrode and the workpiece.

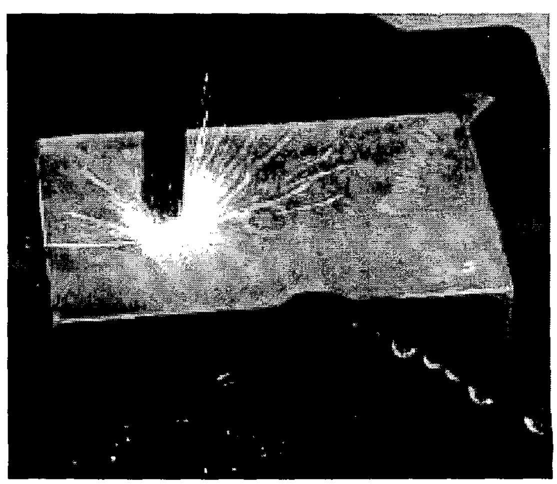

Fig. 12. Close up view of the machining.

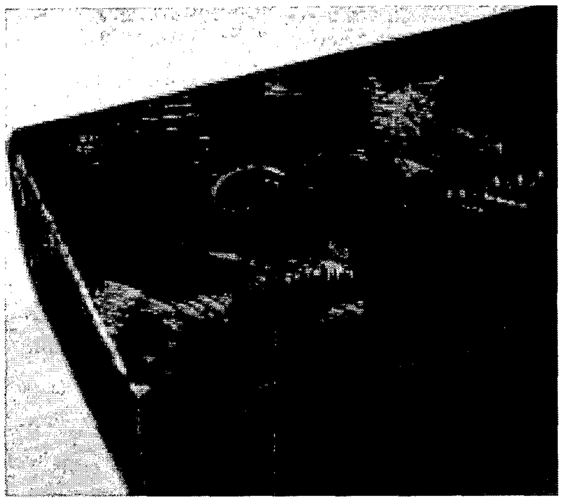

Fig. 13. Cuts in the stainless steel workpiece.

VI. CONCLUSIONS

A new application for resonant converters such as EDM power supplies has been proposed. This proposal results in a great reduction in weight and size being specially suitable for portable operations. This technology, firstly oriented to underwater operations in nuclear plants might be extended for chip-less metal machining at low cost. The design specifications of an LCC resonant converter for an EDM application have been established. The design strategy imposes a nominal operating point where the converter behaves as a current source and so the conditions for a current source mode have been defined. The performance of a practical implementation of the converter has been verified by loading the circuit with: 1) the nominal resistance that models the arc, 2) a resistance that models an overload of 50% and 3) under short-circuit conditions. First experiments have been carried out on a EDM system and the prototype of the LCC converter has been proved to be well suited to fulfill the EDM requirements with the addition of further performances regarding efficiency and current stability under very irregular load conditions. Further work is in progress to characterize the resulting EDM process parameters such as metal removal rate, surface finish and electrode wear.

VII. ACKNOWLEDGMENT

This work has been carried out under the initiative of the company “ENWESA Operaciones”, and it has received financial support from the “Fondos FEDER” of the European Union.

VIII. REFERENCES

[1] G. Boothroyd, W. A. Knight, *Fundamentals of Machining and Machine Tools.* 2nd Edition. New York: Marcel Dekker, 1989.

[2] E. Bud Guitrau, *The EDM Handbook.* Hanser Gardner Publications, 1997.

[3] Electrical Discharge Machining; concepts, methods, applications. Standard VDI 3400. June 1975.

[4] R. L. Steigerwald. “A Comparison of Half-Bridge Resonant Converter Topologies”, *IEEE Transactions on Power Electronics*, Vol. 3, No. 2, April 1988, pp. 174-182.

[5] Marian K. Kazimierczuk, Dariusz Czarkowski, *Resonant Power Converters.* New York: Wiley Interscience Publication, 1995.

[6] Rosario Casanueva, Manuel Ochoa, Francisco J. Azcondo, Salvador Bracho “Current Mode Controlled LCC Resonant Converter for Electrical Discharge Machining Applications”, in *Proceedings of the 2000 IEEE International Symposium on Industrial Electronics*, 00TH8543, Vol. 2, Dec. 2000, pp. 505-510.